physica status solidi a
www.pss-a.com

Check for updates

Magnetic Field Effect in Hydrogen-Bonded Semiconductor-Based Organic Field-Effect Transistors

*Donia Saadi, Cigdem Yumusak, Ivana Zrinski, Andrei Ionut Mardare, Samir Romdhane, Niyazi Serdar Sariciftci, Mihai Irimia-Vladu, and Markus Clark Scharber**

Herein, the magnetic field effect on the source–drain current of organic field-effect transistors with semiconductor layers made of H-bonded pigments is studied. In all devices, an external magnetic field reduces the source–drain current in the transistor. The magnetic field effect is independent of the direction of the applied magnetic field. The observed increase of the magnetoresistance seems to originate from the used semiconductor or the semiconductor–dielectric interface and is not influenced by the nature of the gate electrodes or the semiconductors' deposition procedure (e.g., grain size, layer thicknesses, etc.). As all prepared devices do have single charge carrier nature, the formation of bipolarons is suggested to be responsible for the observed magnetic field effect. The presented experiments demonstrate that hydrogen-bonded semiconductors behave no different than their classical van der Waals-bonded fully conjugated semiconductors' counterparts.

1. Introduction

H-bonded pigments (HBPs) have attracted a lot of attention in recent years due to their interesting optical and electronic properties.[1–5] The main advantages of HBPs are their simple chemistry, their availability on large scale, and their low costs. Quinacridone (QA) nanocrystallites, for example, form the magenta toner often found in inkjet printers, whereas epindolidione (EPI) is currently applied as a yellow colorant in different ink formulations.[6–8] Many HBPs are of natural origin and are based on hydrogen-bonded π-stacked organic solids.[9] Semiconducting HBPs can be found among others in the indigo family.[10,11] Also, the five-ring QA and the four-ring EPI, the hydrogen-bonded analogs of the well-known organic semiconductors pentacene and tetracene, allow the preparation of stable and well-performing field-effect transistors, light-emitting diodes, and even homojunction photovoltaic cells.[1,12–14] The mechanism of charge transport in HBPs is rather peculiar and rests on the existence of the hydrogen bond itself; due to hydrogen bonding, in the solid state, the HBP molecules strongly interact with one another and form pigment particles with markedly different optical and charge transport properties compared to isolated molecules.[15,16]

Up to now, not only the performance of H-bonded-based semiconductor devices but also the stability of such devices under operation in air, under electrical bias stress, or at various elevated temperature exposures were reported.[17–19] The goal of the work summarized in this article was to gain a deeper understanding of the charge transport processes in HBPs in the presence of a magnetic field. To the best of our knowledge, there was so far no attempt to quantify the magnetic response of HBP semiconductors under operation in electronic devices. With this respect, we selected here the organic field-effect transistor (OFET) as the working horse device for our investigations.

Magnetic field effects (MFEs) in organic semiconductors have been known for a long time.[20,21] Despite the absence of magnetic elements, relatively small magnetic B-field strengths of only a few millitesla can manipulate the photoluminescence, the magnetotransport properties, and the density of excited states in this material class.[21,22] Studying the magnetic effect gives insights into the microscopic processes in organic semiconductors including the interaction between species carrying spin and their molecular environment. Several mechanisms have been discussed for the observed MFEs.[22,23] Among the proposed mechanisms are the recombination of free charges and the formation

D. Saadi, C. Yumusak, N. S. Sariciftci, M. Irimia-Vladu, M. C. Scharber
Institute of Physical Chemistry
Linz Institute for Organic Solar Cells
Johannes Kepler University Linz
Altenberger Straße 69, 4040 Linz, Austria
E-mail: markus_clark.scharber@jku.at

D. Saadi, S. Romdhane
Laboratoire Matériaux Avancés et Phénomènes Quantiques
Faculté des Sciences de Tunis
Université de Tunis El Manar
Campus Universitaire, Tunis 2092, Tunisia

I. Zrinski, A. I. Mardare
Institute of Chemical Technologies of Inorganic Materials
Johannes Kepler University Linz
Altenberger Straße 69, 4040 Linz, Austria

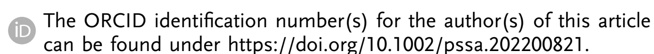
The ORCID identification number(s) for the author(s) of this article can be found under https://doi.org/10.1002/pssa.202200821.

© 2023 The Authors. physica status solidi (a) applications and materials science published by Wiley-VCH GmbH. This is an open access article under the terms of the Creative Commons Attribution-NonCommercial License, which permits use, distribution and reproduction in any medium, provided the original work is properly cited and is not used for commercial purposes.

DOI: 10.1002/pssa.202200821

© 2023 The Authors. physica status solidi (a) applications and materials science published by Wiley-VCH GmbH

18626319, 0, Downloaded from https://onlinelibrary.wiley.com/doi/10.1002/pssa.202200821 by Johannes Kepler Universität Linz, Wiley Online Library on [09/03/2023]. See the Terms and Conditions (https://onlinelibrary.wiley.com/terms-and-conditions) on Wiley Online Library for rules of use; OA articles are governed by the applicable Creative Commons License

of polaron pairs,[24] the intersystem crossing between singlet and triplet states, the population of triplet states, and the interaction between triplets or a polaron and a triplet state.[22,24] All these processes can be manipulated by an external magnetic field. So far, the MFE has mainly been analyzed in vertically two-terminal devices such as light-emitting diodes and solar cells.[21] To gain a deeper understanding of microscopic processes, it is important to study the MFE also in OFETs. These three-terminal devices allow precise control of the charge carrier density and the type of mobile charge carrier present in the transistor channel. In OFETs, MFE has been observed in unipolar and ambipolar devices.[25,26] The source–drain current of the devices can be altered with a magnetic field, which is often discussed in the framework of an MFE of the resistance of the transistor channel. While ambipolar transistors do exhibit a positive and a negative magnetoresistance (MR), in unipolar OFETs an external magnetic field increases the resistance (positive MR) of the device. As all materials including the gate used in OFETs are often made of nonmagnetic materials, the MFE has been attributed to a field-induced modulation of the charge carrier density and/or to changes in the charge carrier mobility. Due to the unipolar character of the charge transport in typical OFETs, only electrons or holes are present in the conducting channel and no polaron pairs or excitons can be formed. To explain the MFEs observed in these single-carrier devices, the so-called bipolaron model has been proposed.[27–30] It relies on the spin-dependent formation of double-occupied molecular states (bipolarons) during hopping transport in disordered organic semiconductors. The bipolaron formation is magnetic field dependent and results in a positive MR. Here, we investigate the MFE on OFETs based on the HBPs *N*,*N′*-dimethyl quinacridone (DMQA), QA, and EPI. All investigated devices show the typical characteristics of unipolar transistors and no superlinear increase of I_{DS} was observed on the OFETs used in this study. We find a positive MR in the prepared unipolar p-type devices. In addition, an applied magnetic field can shift the gate voltage and reduces the hysteresis observed in the transfer characteristic of the transistors.

2. Experimental Section

The chemical structures of the used pigments are shown in **Figure 1**a. All the examined small molecules in this study were subjected to scrupulous purification processes, by methods reported earlier.[31] Each of the three HBPs has been purified by two successive temperature gradient sublimations. Bottom gate–top contact OFETs were fabricated on borosilicate glass substrates, with a channel length, $L = 25\,\mu m$, and width, $W = 2\,mm$. The OFET design is shown in Figure 1b.[32] The top surface of the aluminum gate electrode (≈80 nm thickness) was electrochemically and superficially anodized to Al_2O_3 by a method reported earlier to form about 18 nm-thick aluminum oxide layer.[33,34] To investigate the role of the gate material, also Hf/HfO_2 gate structures were prepared. Hafnium films with a thickness of 85 nm were deposited on borosilicate glass substrates by magnetron sputtering. For this purpose, a high-purity target (99.9% metals basis excluding Zr) with a diameter of 50 mm was used in an ultrahigh vacuum system (Mantis Deposition, UK) with a base pressure in the range of 10^{-7} Pa. The sputtering process was performed in direct current mode using a power of 49 W with a deposition rate of $2.3\,nm\,min^{-1}$. The deposition by sputtering of Hf and Hf-based layers represents an excellent technique for the production of high-quality metallic thin film electrodes for a variety of applications.[35–37] Immediately after deposition, the Hf gate films were transferred by a robotic arm without breaking the vacuum into a self-developed scanning energy dispersive X-ray spectroscopy (EDX) system attached to the same vacuum chamber cluster. The system was designed for thin and ultrathin film analysis by removing the final electron aperture of the electron gun, allowing illumination spots of 0.5 mm in diameter. This extremely large area of electron irradiation (compared to commercially available systems where nm^2 is analyzed) leads to an increased photon signal/noise ratio dramatically improving the possibilities of compositional analysis in films. Additionally, X-ray photoelectron spectroscopy (XPS) was used for the surface analysis of the gate oxides and for

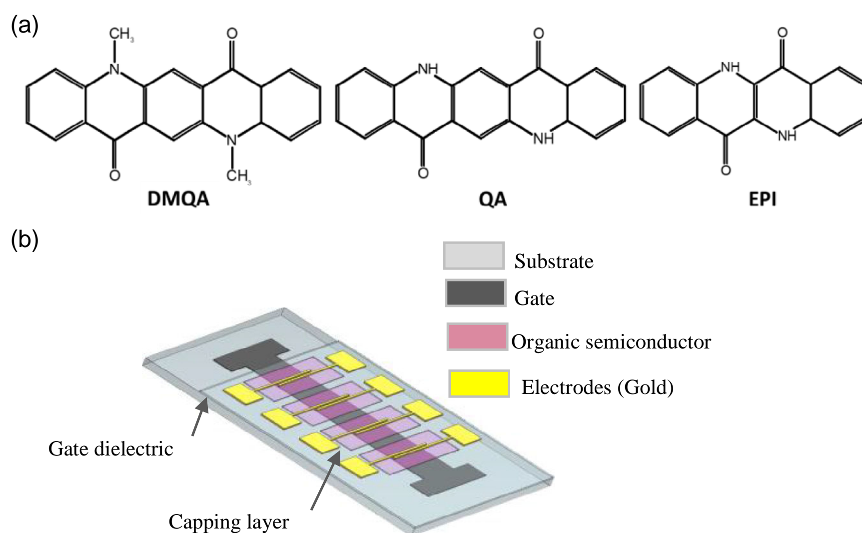

Figure 1. a) Chemical structure of the *N*,*N′*-dimethyl quinacridone (5,12-dimethylquinolino[2,3-b]acridine-7,14-dione (DMQA), QA, and EPI; b) OFETs device geometry in the bottom gate–top contact configuration of our laboratory.

© 2023 The Authors. physica status solidi (a) applications and materials science published by Wiley-VCH GmbH

18626319, 0, Downloaded from https://onlinelibrary.wiley.com/doi/10.1002/pssa.202200821 by Johannes Kepler Universität Linz, Wiley Online Library on [09/03/2023]. See the Terms and Conditions (https://onlinelibrary.wiley.com/terms-and-conditions) on Wiley Online Library for rules of use; OA articles are governed by the applicable Creative Commons License

confirming the EDX results. The gate Hf thin film was electrochemically anodized to HfO_2 under ambient conditions to form about 16–20 nm of the gate oxide, similar to previous studies.[38,39] Anodic oxide was grown potentiodynamically in citrate buffer electrolyte which was prepared according to standard protocols.[40] Cyclic voltammograms were recorded for samples by increasing the potential to 8 V (relative to the standard hydrogen electrode [SHE]) and then back to 0 V. We used in this process a potentiostat (CompactStat Ivium, The Netherlands) connected to a three-electrode cell in which 0.5 mm-thick graphite foil served as the counter electrode, Hg/Hg_2SO_4/sat. K_2SO_4 electrode (0 V vs $Hg/Hg_2SO_4 = 0.640$ V vs SHE) was used as the reference electrode and Hf film served as the working electrode. If not mentioned otherwise, a 20 nm of aliphatic tetratetracontane (TTC) capping layer was vacuum deposited on top of the aluminum oxide layer at a deposition rate between 0.7 and 1 $Å\,s^{-1}$ in a physical vapor deposition (PVD) system, followed by in situ annealing for 30 min at 65 °C in a vacuum before the semiconductor deposition that was performed without interrupting the vacuum. As an alternative interfacial material beeswax was applied as a hydrophobic capping layer, ≈12 nm of this material was doctor bladed from 2 $mg\,mL^{-1}$ solution in chloroform.[41]

The three HBP semiconductors (schematically displayed in Figure 1a) were deposited by thermal evaporation at a pressure of 1×10^{-6} mbar with a deposition rate of either 0.1–0.2 $Å\,s^{-1}$ (slow) or 4–5 $Å\,s^{-1}$ (fast). The samples were directly transferred from the vacuum chamber to a nitrogen-filled glove box (with levels of O_2, and H_2O below 0.1 ppm) where gold (Au) source and drain electrodes were deposited on the channel via physical vapor deposition. For the MR measurements, the specimen was placed on a sample holder and fixed between the poles of an electromagnet. The wires were bonded to the electrodes with small pieces of indium and they were connected to a probe station. A magnetic field was applied parallel and perpendicular to the direction of the OFET current, with the OFET being placed in three alternative positions, as presented in **Figure 2**. The current–voltage measurements were measured using Agilent EasyEXPERT program when the magnetic field was varied between 0 and 1 T. All the measurements were performed in the dark and at room temperature (≈293 K).

3. Results and Discussion

Figure 3a shows a typical transfer characteristic of an OFET with a DMQA semiconductor layer and aluminum/aluminum oxide (Al/AlO_x) coated with a TTC as the gate dielectric layers. The black line represents the transfer characteristic when no magnetic field is applied. In red the transfer characteristic of the same transistor is shown when an external magnetic B-field strength of 1 Tesla is applied. The external magnetic field reduces the source–drain current for a wide range of gate voltages. In Figure 3b, the output characteristics recorded at different gate voltages either without or with an external magnetic field are shown: solid color lines indicate when the magnetic field is not present and dashed color lines show the output characteristics when 1 T of the external magnetic field is applied with keeping parity color for without/with a magnetic field. In the presence of a magnetic field, I_{DS} is reduced significantly, as shown in Figure 3b. To test the effect of the direction of the magnetic field on source–drain (I_{DS}) current, the OFET transistors were mounted in three different orientations in the used electromagnet (Figure 2). For all investigated devices, we could not find any influence of the magnetic field direction on the MFE. Figure 3c shows the change of the MR ratio measured with $V_{gs} = -8$ V and $V_{DS} = -5$ V. MR is calculated using

$$\mathrm{MR}(B) = \frac{R(B) - R(0)}{R(0)} \tag{1}$$

where R is the resistance of the transistor channel with and without a magnetic field. MR increases quickly at low magnetic fields and saturates at higher fields.

Figure 3d shows the MR at different gate voltages, at a constant source–drain voltage, and at different external magnetic fields. The MR is largest at low gate voltages and decreases with decreasing V_{gs}

We also prepared transistors in the standard layout using EPI and unsubstituted QA as semiconductor materials. Both materials have been used successfully in stable and well-performing OFETs.[12,17,18,19,32] In **Figure 4**, the transfer and output characteristics and the MR of an EPI-based OFET recorded at a constant source–drain voltage and different gate voltages are shown.

In **Figure 5**, the findings for the QA-based OFET are summarized.

To examine possible influences on the magnetic response of the OFETs, we proceeded to investigate the role of the gate material, the interfacial coating of the gate oxide, and the growth conditions of the semiconductor layer. The following transistors based on DMQA were considered for MR effect: a) transistors with a Hf/HfO_x gate coated with tetratetracontane; b) transistors with an Al/AlO_x gate coated with a thin layer of beeswax; and

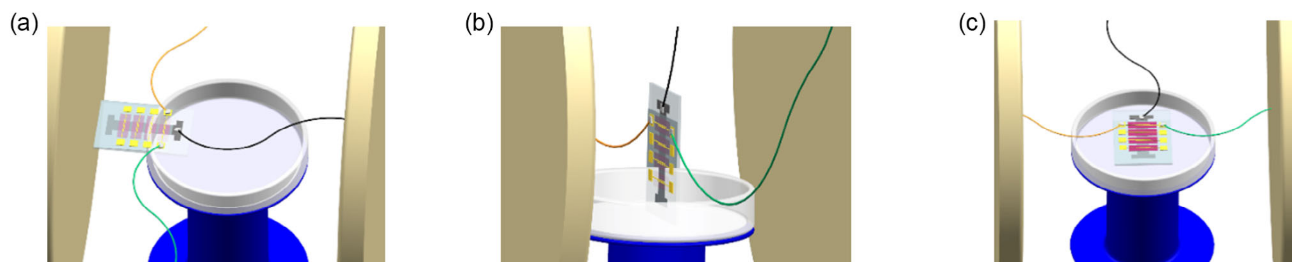

Figure 2. Schematic 3D view of the positions of the device between the poles of an electromagnet: a) first position when the magnetic B-field strength is parallel to the direction of the current flow of the device, from source to drain; b,c) second and third positions, respectively, when the magnetic B-field strength is perpendicular to the source–drain direction of current flow.

© 2023 The Authors. physica status solidi (a) applications and materials science published by Wiley-VCH GmbH

18626319, 0, Downloaded from https://onlinelibrary.wiley.com/doi/10.1002/pssa.202200821 by Johannes Kepler Universität Linz, Wiley Online Library on [09/03/2023]. See the Terms and Conditions (https://onlinelibrary.wiley.com/terms-and-conditions) on Wiley Online Library for rules of use; OA articles are governed by the applicable Creative Commons License

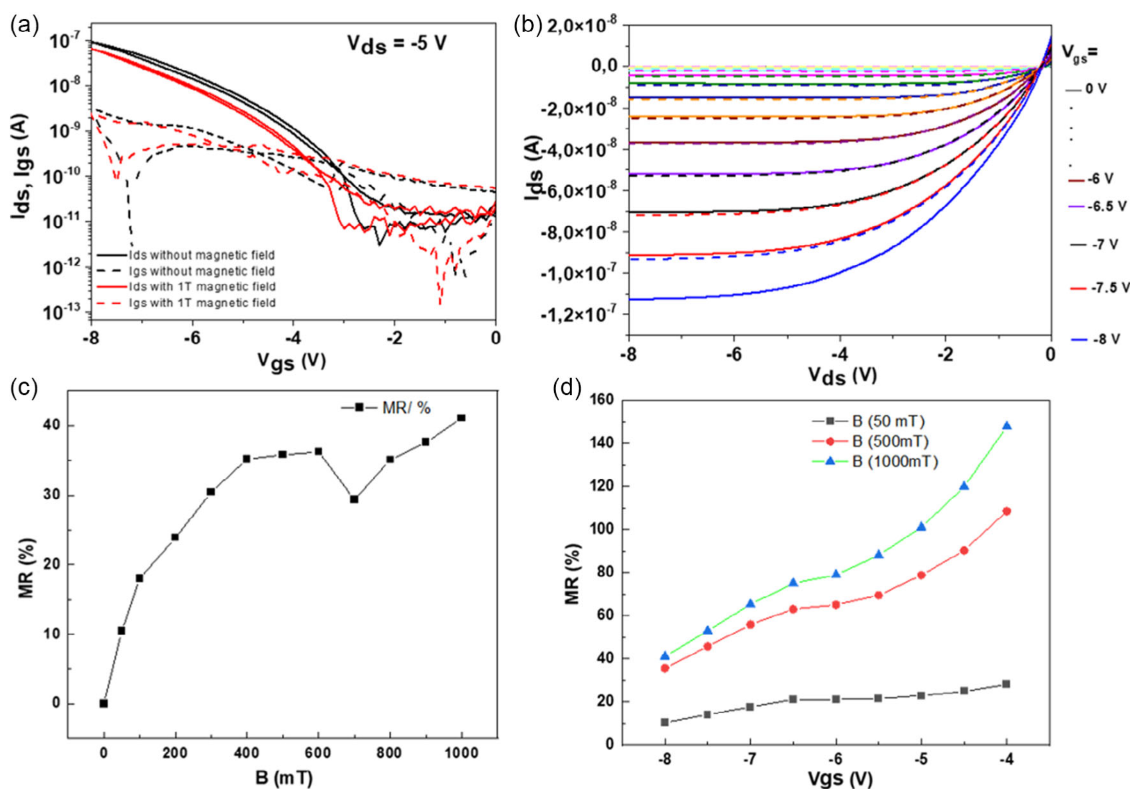

Figure 3. a) AlO_x-gated OFET based on DMQA (deposition rate: 0.1–0.2 Å s^{-1}) transfer characteristics at fixed $V_{DS} = -5$ V; b) output characteristics with (dashed line)/without (solid line) magnetic field; c) MR plotted as a function of magnetic B-field strength measured at $V_{gs} = -8$ V and $V_{DS} = -5$ V; d) MR plotted as a function of V_{gs} at $V_{DS} = -5$ V at $B = 50$, 500, and 1000 mT.

c) transistors with an Al/AlO_x gate coated with tetratetracontane, but DMQA layer was deposited at a faster rate (4–5 Å s^{-1}).

All the devices showed similar behavior in an external magnetic field compared to the standard transistors discussed before (see Figure 1–3). This suggests that the observed MFE is related to the semiconductor material and is not originating from the gate dielectric. In addition, we looked into the composition of the gate/oxide films, as well as the borosilicate glass substrate, to rule out the presence of magnetic species in the layers below the semiconductor. Both EDX and XPS analysis indicated that only pure metals/oxides are present in the films. Apart from the pure metals, Si, O, and small amounts of Ca and Na native to the borosilicate glass were identified. All the above investigations showed unequivocally that the MFE observed in the HBP-based OFETs originates either from the semiconductors themselves, or from the interface of the semiconductors to the dielectric.

In addition, it is worth pointing out that all the presented transistors do not exhibit a sensitivity to the magnetic field direction (i.e., orientation). With this respect, we obtained strikingly similar OFET curves for each of the three semiconductors, irrespective of the orientation of the test samples between the poles of the magnet (shown schematically in Figure 2). In Figure S4, Supporting Information, the transfer characteristics of a DMQA-based transistor, measured at three different magnetic field directions, are shown. For EPI and QA, very similar behaviors were observed. Applying an external magnetic field reduces the source–drain current, leading to an increase in the MR ratio. As all measurements are performed in the dark; only one type of mobile charge carrier is present in the device. In the absence of any photoexcited species including triplet exciton, only the so-called bipolaron mechanism has been proposed to explain the effect of an external magnetic field on the current in a semiconductor. A bipolaron is a (quasi)particle consisting of two equally charged polarons—either two electrons or two holes—on the same molecular site. They can only be formed in the singlet state because the triplet state is much higher in energy and has, therefore, a very small formation rate.[42,43] The bipolaron model describes a situation where a charge carrier is quasistationary trapped at an energetically low-lying state. A nearby free carrier, which would normally contribute to the source to drain (I_{DS}) current, has to pass over this site by—at least as a temporary intermediate state—forming a doubly occupied site, that is, a bipolaron. The spins of two polarons that meet each other are random, so their spin configuration can be either a singlet or a triplet. In the latter case, bipolaron formation is not possible and the current flow through the semiconductor is blocked. However, local magnetic fields will mix their spin configuration, allowing polarons that are initially triplets to form a bipolaron in the singlet configuration. An external magnetic field lifts the degeneracy of the three triplet states and the T^- and T^+ triplets can no longer mix with the singlet. This means that an external magnetic field leads to a lower current as fewer triplet polaron

© 2023 The Authors. physica status solidi (a) applications and materials science published by Wiley-VCH GmbH

18626319, 0, Downloaded from https://onlinelibrary.wiley.com/doi/10.1002/pssa.202200821 by Johannes Kepler Universität Linz, Wiley Online Library on [09/03/2023]. See the Terms and Conditions (https://onlinelibrary.wiley.com/terms-and-conditions) on Wiley Online Library for rules of use; OA articles are governed by the applicable Creative Commons License

18626319, 0, Downloaded from https://onlinelibrary.wiley.com/doi/10.1002/pssa.202200821 by Johannes Kepler Universität Linz, Wiley Online Library on [09/03/2023]. See the Terms and Conditions (https://onlinelibrary.wiley.com/terms-and-conditions) on Wiley Online Library for rules of use; OA articles are governed by the applicable Creative Commons License

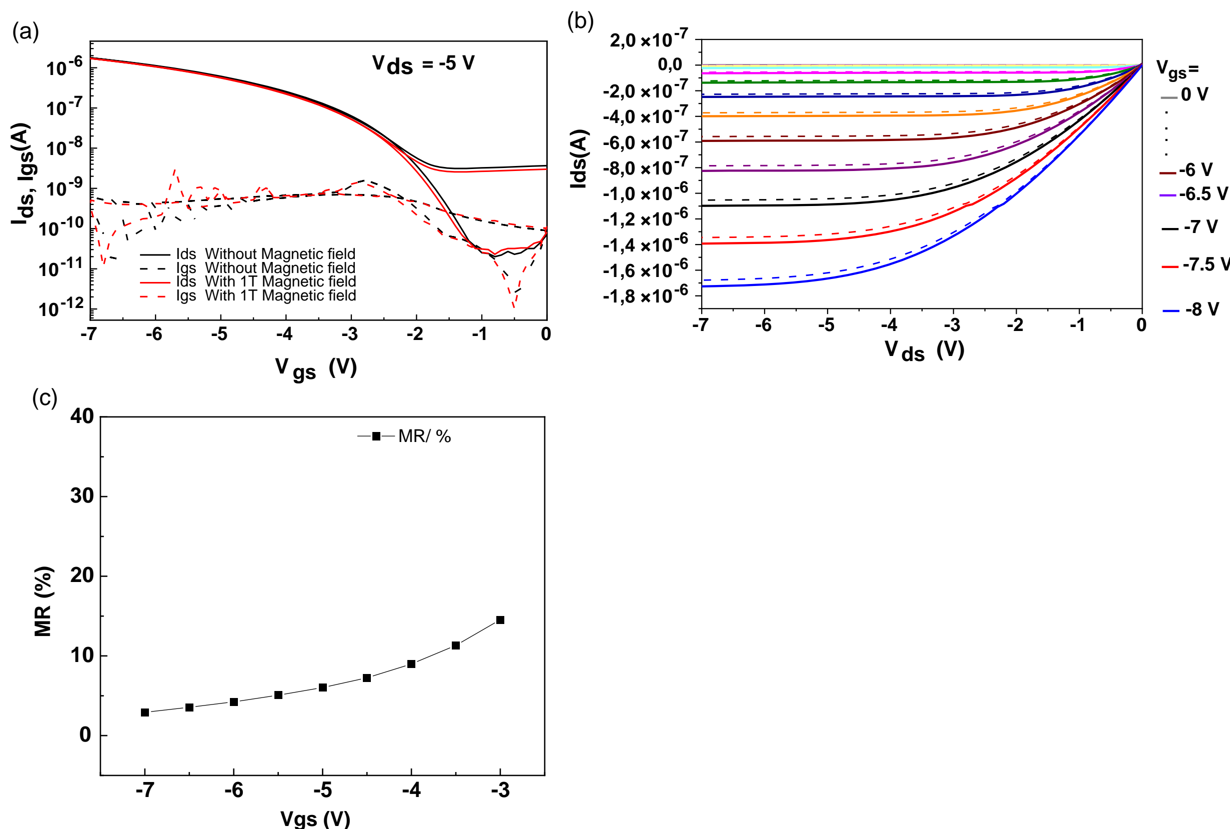

Figure 4. a) Transfer characteristics of AlO_x-OFET with an EPI semiconductor at fixed $V_{DS} = -5$ V recorded with no magnetic B-field strength (black) and 1 T (red) applied; b) output characteristics in (solid line) recorded with no magnetic B-field strength and 1 T (dashed line) are applied; c) MR plotted as a function of V_{gs} at $V_{DS} = -8$ V extracted from (b).

pairs can be converted into singlet bipolarons. Thus, the bipolaron mechanism gives rise to a magnetic field dependence of the charge carrier mobility and leads, in this case, to a positive MR (e.g., a decrease of the measured I_{DS} current, a fact that is consistently observed throughout this work). As the external magnetic field determines the spin polarization of the charge carriers in the semiconductor, it also determines the formation of polaron pairs. The orientation of the transistor or the direction of the transistor current with respect to the external magnetic field plays no role in the discussed bipolaron mechanism, which is in good agreement with our experimental findings.

Assuming that the bipolaron mechanism is dominant in the investigated field-effect transistors, MR is a measure of the defect density in the semiconductor material. Large changes in the MR suggest a large number of defects in the semiconductor leading to a larger number of trapped carriers and a higher probability that a mobile charge carrier is blocked via the bipolaron mechanism. The MFE could also show a gate bias dependence. At high charge carrier densities in the semiconductor, all trap states are filled. A further increase in the charge carrier concentration by increasing the gate bias will not lead to additional trapped polarons required for the bipolaron mechanism and the relative effect of the magnetic field on the current is reduced (see Figure 3d, 4d, and 5d). This is indeed what we have observed in all our experiments: increasing the gate bias reduces the MR in all studied devices.

The change of threshold voltage and the reduction of the transfer characteristic hysteresis observed, e.g., for DMQA-based transistors (Figure 3) are not fully understood. In line with our finding, Street et al.[44] proposed that the formation of bipolarons can also affect the hysteresis of OFETs. Bipolarons are often formed at trapping sites, and their slow trapping and detrapping lead to the observed hysteresis and electrostatic changes at the gate electrode. As discussed above, an applied magnetic field reduces the probability of bipolaron formation and should therefore reduce the hysteresis of the OFET transfer characteristic.

In the literature, MR in molecular systems with very different amplitude has been reported.[27,45,46] At the moment it is not fully understood why some systems exhibit MR changes in the range of 1%,[27] while other systems show MR changes exceeding 1000%.[47] An important theoretical observation is provided by Kersten et al.[48] The authors find that inter- and intrachain transport plays an important role. In addition, traps are believed to influence the MR of a system. These findings suggest that not only the molecular structure but also the device manufacturing affect the behavior of an OFET in an external magnetic field.

4. Conclusion

We have studied the MFE on the source–drain current of OFETs based on the HBPs N,N'-dimethyl quinacridone, EPI, and QA. In

© 2023 The Authors. physica status solidi (a) applications and materials science published by Wiley-VCH GmbH

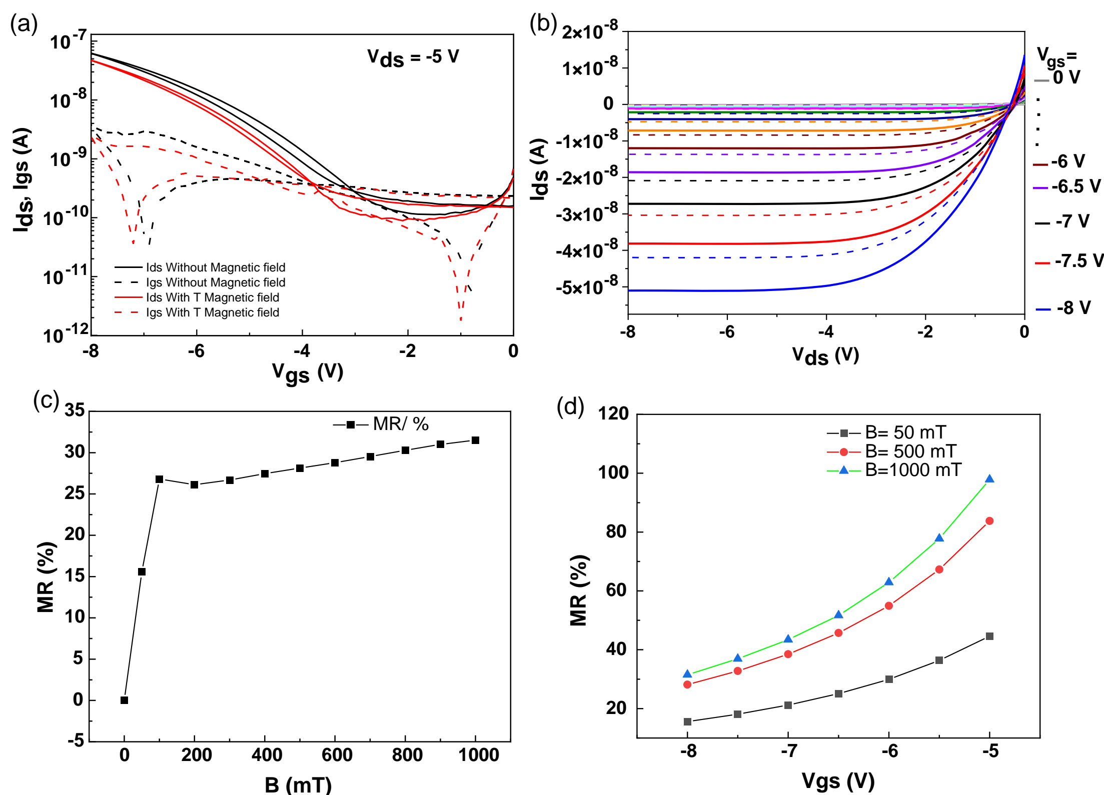

Figure 5. a) Transfer characteristics of an OFET based on QA, operating in a voltage window of −8 V at an applied V_{DS} of −5 V; b) output characteristics with/without magnetic field; c) MR plotted as a function of magnetic B-field strength when $V_{gs} = -8$ V, $V_{ds} = -5$ V; d) MR plotted as a function of V_{gs} (V), at different applied magnetic B-field strength $B = 50$, 500, and 1000 mT at $V_{DS} = -5$ V.

all devices, an external magnetic field reduces the source–drain current in the transistors. The MFE is independent of the direction of the applied magnetic field. In line with the observations of the scientific community, the formation of bipolarons is suggested to be responsible for the observed MFE and it may also explain the reduced hysteresis and threshold voltage shift observed in some of the prepared transistors. Our work demonstrates that hydrogen-bonded semiconductors behave no different than their counterparts, the classic, van der Waals-bonded semiconductors, when subjected to a magnetic field in OFET devices. Also, the observed magnetic response of all the investigated OFETs seems to originate from the semiconductors or semiconductors to dielectric(s) interface and is not influenced by the nature of the gate electrodes.

Supporting Information

Supporting Information is available from the Wiley Online Library or from the author.

Acknowledgements

The authors thank the Austrian Agency for International Cooperation in Education and Research (OEAD-GmbH, WTZ, CZ01/2020, 8J20AT025) and the Austrian "Climate and Energy Fund" within the program Energy Emission Austria (Project: ALTAFOS, FFG No. 865072) for financial support.

Conflict of Interest

The authors declare no conflict of interest.

Data Availability Statement

The data that support the findings of this study are available from the corresponding author upon reasonable request.

Keywords

field-effect transistors, magnetic field, organic semiconductors

Received: November 27, 2022
Revised: January 13, 2023
Published online:

[1] H. Jiang, S. Zhu, Z. Cui, Z. Li, Y. Liang, J. Zhu, P. Hu, H.-L. Zhang, W. Hu, *Chem. Soc. Rev.* **2022**, *51*, 3071.
[2] Y. Zhang, W. Wang, *Comput. Theor. Chem.* **2021**, *1194*, 113074.
[3] P. Gómez, S. Georgakopoulos, M. Más-Montoya, J. Cerdá, J. Pérez, E. Ortí, J. Aragó, D. Curiel, *ACS Appl. Mater. Interfaces* **2021**, *13*, 8620.
[4] T. Maeda, A. Liess, A. Kudzus, A.-M. Krause, M. Stolte, H. Amitani, S. Yagi, H. Fujiwara, F. Würthner, *Chem. Commun.* **2020**, *56*, 9890.
[5] M. Koehler, D. Farka, C. Yumusak, N. S. Sariciftci, P. Hinterdorfer, *ChemPhysChem* **2020**, *21*, 659.
[6] S. S. Labana, L. L. Labana, *Chem. Rev.* **1967**, *67*, 1.

© 2023 The Authors. physica status solidi (a) applications and materials science published by Wiley-VCH GmbH

18626319, 0, Downloaded from https://onlinelibrary.wiley.com/doi/10.1002/pssa.202200821 by Johannes Kepler Universität Linz, Wiley Online Library on [09/03/2023]. See the Terms and Conditions (https://onlinelibrary.wiley.com/terms-and-conditions) on Wiley Online Library for rules of use; OA articles are governed by the applicable Creative Commons License

[7] S. Magdassi, in *The Chemistry of Inkjet Inks*, World Scientific Publishing Co, Singapore **2010**.
[8] B. Lal, K. Bruno, P. Valérie, W. Frank, P. Martin, U. Schmidt, US Patent 7307170B2.
[9] H. Zollinger, in *Color Chemistry: Syntheses, Properties, and Applications of Organic Dyes and Pigments*, 3rd ed., Wiley-VCH, Weinheim **2003**.
[10] E. D. Glowacki, G. Voss, L. N. Leonat, M. Irimia-Vladu, S. Bauer, N. S. Sariciftci, *Isr. J. Chem.* **2012**, *52*, 540.
[11] M. Irimia-Vladu, E. D. Glowacki, P. A. Troshin, D. K. Susarova, O. Krystal, G. Schwabegger, M. Ullah, Y. Kanbur, M. A. Bodea, V. F. Razumov, H. Sitter, S. Bauer, N. S. Sariciftci, *Adv. Mater.* **2012**, *24*, 375.
[12] E. D. Głowacki, G. Romanazzi, C. Yumusak, H. Coskun, U. Monkowius, G. Voss, M. Burian, R. T. Lechner, N. Demitri, H. J. Redhammer, N. Sünger, G. P. Suranna, N. S. Sariciftci, *Adv. Funct. Mater.* **2015**, *25*, 776.
[13] E. D. Glowacki, L. Leonat, M. Irimia-Vladu, R. Schwödiauer, M. Ullah, H. Sitter, S. Bauer, N. S. Sariciftci, *Appl. Phys. Lett.* **2012**, *101*, 023305.
[14] S. Dunst, E. Karner, M. E. Coppola, G. Trimmel, M. Irimia-Vladu, *Monats. Chem.* **2017**, *148*, 863.
[15] G. Lincke, *Dyes Pigments* **2002**, *52*, 169.
[16] V. Coropceanu, J. Cornil, D. A. da Silva Filho, Y. Olivier, R. Silbey, J.-L. Brédas, *Chem. Rev.* **2007**, *107*, 926.
[17] E. D. Głowacki, M. I. Vladu, M. Kaltenbrunner, J. Gsiorowski, M. S. White, U. Monkowius, G. Romanazzi, G. P. Suranna, P. Mastrorilli, T. Sekitani, S. Bauer, T. Someya, L. Torsi, N. S. Sariciftci, *Adv. Mater.* **2013**, *25*, 1563.
[18] M. Irimia-Vladu, Y. Kanbur, F. Camaioni, C. Yumusak, A. A. Vlad, C. V. Irimia, A. Operamolla, G. Farinola, G. Romanazzi, G. P. Suranna, N. González, M. C. Molina, L. F. Bautista, H. Langhals, E. D. Glowacki, N. S. Sariciftci, *Chem. Mater.* **2019**, *31*, 6315.
[19] Y. Kanbur, H. Coskun, E. D. Głowacki, M. Irimia-Vladu, N. S. Sariciftci, C. Yumusak, *Org. Electron.* **2019**, *66*, 53.
[20] R. H. Clarke, R. E. Connors, J. Keegan, *J. Chem. Phys.* **1977**, *66*, 358.
[21] M- Wohlgenannt, *World Scientific Reference on Spin in Organics*, Materials and Energy, Vol. *3*, World Scientific, Singapore **2018**.
[22] U. E. Steiner, T. Ulrich, *Chem. Rev.* **1989**, *89*, 51.
[23] P. Janssen, M. Cox, S. H. P. Wouters, M. Kemerink, M. M. Wienk, B. Koopmans, *Nat. Commun.* **2013**, *4*, 2286.
[24] V. Dyakonov, E. Frankevich, *Chem. Phys.* **1998**, *227*, 203.
[25] E. Tatarov, T. Reichert, T. P. I. Saragi, A. Scheffler, R. Ueberschaer, C. Bruhn, T. Fuhrmann-Lieker, J. Salbeck, *Chem. Commun.* **2013**, *49*, 4564.
[26] C. Reichert, Organische Magnetooptoelektronik, Ph.D. Thesis, University of Kassel, **2014**
[27] W. Wagemans, B. Koopmans, *Phys. Status Solidi* **2011**, *248*, 1029.
[28] B. Hu, L. Yan, M. Shao, *Adv. Mater.* **2009**, *21*, 1500.
[29] P. A. Bobbert, T. D. Nguyen, F. W. A. van Oost, B. Koopmans, M. Wohlgenannt, *Phys. Rev. Lett.* **2007**, *99*, 216801.
[30] W. Wagemans, P. Janssen, A. J. Schellekens, F. L. Bloom, P. A. Bobbert, B. Koopmans, *Spin* **2011**, *01*, 93.
[31] C. Yumusak, N. S. Sariciftci, M. Irimia-Vladu, *Mater. Chem. Front.* **2020**, *4*, 3678.
[32] J. Ivić, A. Petritz, C. V. Irimia, B. Kahraman, Y. Kanbur, M. Bednorz, C. Yumusak, M. A. Aslam, A. Matković, K. Saller, C. Schwarzinger, W. Schühly, A. I. Smeds, Y. Salinas, M. Schiek, F. Mayr, C. Xu, C. Teichert, M. Osiac, N. S. Sariciftci, B. Stadlober, M. Irimia-Vladu, *Adv. Sust. Syst.* **2022**, *6*, 2270029.
[33] M. Irimia-Vladu, N. Marjanovic, M. Bodea, G. Hernandez-Sosa, A. Montaigne Ramil, R. Schwödiauer, S. Bauer, N. S. Sariciftci, F. Nüesch, *Org. Electron.* **2009**, *10*, 408.
[34] M. Kaltenbrunner, P. Stadler, R. Schwödiauer, A. W. Hassel, N. S. Sariciftci, S. Bauer, *Adv. Mater.* **2011**, *23*, 4892.
[35] L. Khomenkova, C. Dufour, P.-E. Coulon, C. Bonafos, F. Gourbilleau, *Nanotechnology* **2010**, *21*, 095704.
[36] I. Zrinski, A. Minenkov, C. C. Mardare, J. P. Kollender, S. A. Lone, A. W. Hassel, A. I. Mardare, *Appl. Surf. Sci.* **2021**, *565*, 150608.
[37] M. Braic, M. Balaceanu, A. Vladescu, C. N. Zoita, V. Braic, *Thin Solid Films* **2011**, *519*, 4092.
[38] A. I. Mardare, A. Ludwig, A. Savan, A. D. Wieck, A. W. Hassel, *Sci. Technol. Adv. Mater.* **2014**, *15*, 015006.
[39] A. I. Mardare, C. M. Siket, A. Gavrilovi´c-Wohlmuther, C. Kleber, S. Bauer, A. W. Hassel, *J. Electrochem. Soc.* **2015**, *162*, E30.
[40] *Sodium Phosphate*, Cold Spring Harb. Protoc., **2006**, pdb.rec8303, https://doi.org/org/10.1101/pdb.rec8303.
[41] D. Saadi, F. Mayr, C. Yumusak, D. Wielend, B. Kahraman, C. V. Irimia, Y. Kanbur, M. Bednorz, K. Kotwica, A. ben Fredj, S. Romdhane, M. C. Scharber, N. S. Sariciftci, M. Irimia-Vladu, Unpublished.
[42] M. N. Bussac, L. Zuppiroli, *Phys. Rev. B* **1993**, *47*, 5493.
[43] O. Chauvet, A. Sienkiewicz, L. Forro, L. Zuppiroli, *Phys. Rev. B* **1995**, *52*, R13118.
[44] R. A. Street, A. Salleo, M. L. Chabinyc, *Phys. Rev. B* **2003**, *68*, 085316.
[45] H. Gu, X. Zhang, H. Wei, Y. Huang, A. Wei, Z. Guo, *Chem. Soc. Rev.* **2013**, *42*, 5907.
[46] M. Gobbi, E. Orgiu, *J. Mater. Chem. C* **2017**, *5*, 5572.
[47] Y. Wang, K. Sahin-Tiras, N. J. Harmon, M. Wohlgenannt, M. E. Flatté, *Phys. Rev. X* **2016**, *6*, 011011.
[48] S. P. Kersten, S. C. J. Meskers, P. A. Bobbert, *Phys. Rev. B* **2012**, *86*, 045210.

© 2023 The Authors. physica status solidi (a) applications and materials science published by Wiley-VCH GmbH

18626319, 0, Downloaded from https://onlinelibrary.wiley.com/doi/10.1002/pssa.202200821 by Johannes Kepler Universität Linz, Wiley Online Library on [09/03/2023]. See the Terms and Conditions (https://onlinelibrary.wiley.com/terms-and-conditions) on Wiley Online Library for rules of use; OA articles are governed by the applicable Creative Commons License